*J. Fluid Mech.* (1991), *vol.* 223, *pp.* 93–111
*Printed in Great Britain*



# Asymptotic analysis of the fully developed region of an incompressible, free, turbulent, round jet

By W. B. BUSH[1] AND L. KRISHNAMURTHY[2]
[1] King, Buck & Associates, Inc., San Diego, CA 92110, USA
[2] Florida Institute of Technology, Melbourne, FL 32901–6988, USA

(Received 29 June 1989 and in revised form 2 April 1990)

The structure of the far-field turbulent region of an incompressible free jet developing downstream of an axisymmetric nozzle is studied by means of the Reynolds time-averaged equations. The analysis employs the method of matched asymptotic expansions, with limit-process expansions developed in the limit of large Reynolds number. The analysis reveals the existence, far downstream of the nozzle exit, of a turbulent core region, an irrotational exterior region, and a distinguished intermediate region. Self-similar formulations are sought for all three regions in terms of appropriate independent and dependent variables. The stress- and pressure-function solutions for the exterior region, unlike the mean-velocity solutions, represent new information on the far-field flow behaviour. The analytical results of the centreline decay of the mean axial velocity and those of the radial distributions of the axial and radial mean-velocity components and the shear- and normal-stress components are compared with available experimental data.

## 1. Introduction

The self-similar turbulent round jet, because it is a relatively simple turbulent shear flow, has been the subject of extensive study, both theoretical (see e.g. Abramovich 1963; Hinze 1975; Townsend 1976; Schlichting 1979), and experimental (see e.g. Reichardt 1941; Hinze & Van der Hegge Zijnen 1949; Wygnanski & Fiedler 1969). From the earliest study (Tollmien 1926) up to the present, the (classical) theoretical approach has been to concentrate on the leading-order approximation of the boundary-value problem for the downstream core region to determine the solutions for the mean velocity and the turbulent shear stress.

This paper presents a theoretical study of the structure of a turbulent incompressible, isothermal jet issuing from an axisymmetric nozzle. Attention is directed to the flow-field region far enough downstream of the nozzle exit that there is no residual effect of the initial conditions and self-similarity is attained. In particular, by means of a higher-order asymptotic analysis of the Reynolds time-averaged equations and complementary boundary conditions, presented in §2, the uniformly valid behaviour of the flow quantities, from the jet centreline to the ambient far field, is determined for this downstream self-similar region (see table 1).

In §3, through the consideration of higher-order approximations of the boundary-value problem, in conjunction with the modelling of the experimental data, the solutions for the turbulent normal stresses and the mean pressure in the core region are also ascertained. This higher-order analysis establishes that the resulting core-region solutions are not uniformly valid at the outer edge of this region. To obtain a uniformly valid picture of the flow field, it is necessary to introduce, in addition to

AMBIENT

EXTERIOR REGION

$$x_s = \delta X, \quad r_s = \delta R: \quad \zeta = r_s/x_s = R/X;$$
$$\Psi = \psi_s: \quad U = \delta^2 u_s, \quad V = \delta^2 v_s, \quad \Omega = \delta^3 \omega_s,$$
$$P = \delta^4 p_s, \quad T = \delta^4 \tau_s, \quad M = \delta^4 \mu_s, \quad N = \delta^4 \nu_s.$$

INTERMEDIATE REGION

$$x_k = \delta X, \quad r_k = \delta^{\frac{1}{2}} R: \quad \theta = r_k/x_k = \delta^{-\frac{1}{2}} R/X;$$
$$\Psi = A_0 x_k + \delta \psi_k: \quad U = \delta^2 u_k, \quad V = -\delta^{\frac{3}{2}} A_0 r_k^{-1} + \delta^{\frac{5}{2}} v_k, \quad \Omega = \delta^{\frac{5}{2}} \omega_k,$$
$$P = \delta^3 p_k, \quad T = \delta^{\frac{7}{2}} \tau_k, \quad M = \delta^3 \mu_k, \quad N = \delta^3 \nu_k.$$

CORE REGION

$$x = \delta X, \quad r = R: \quad \eta = r/x = \delta^{-1} R/X;$$
$$\Psi = \psi: \quad U = u, \quad V = \delta v, \quad \Omega = \omega,$$
$$P = \delta p, \quad T = \delta \tau, \quad M = \delta \mu, \quad N = \delta \nu.$$

JET CENTRELINE

TABLE 1. The asymptotic structure of the flow quantities

the downstream core region, a downstream exterior region, at the outer edge of which the flow quantities attain their ambient values; and a downstream intermediate region, in which the flow changes from a core-region-like flow to an exterior-region-like one.

The far-field aspects of jet flow are not often discussed in the literature. Landau & Lifshitz (1959) determine the 'mean flow in the jet outside the turbulent region', which (roughly) corresponds to the downstream exterior region. In §5, the appropriate scaling of the variables indicates that, to leading order of approximation, the exterior region is a turbulent region: the flow is irrotational, yet there is a convection–pressure-gradient–turbulent-stress balance in both the axial and the radial momentum equations. Whereas the resulting mean-velocity solutions are essentially the ones determined by Landau & Lifshitz, the exterior-region stress- and pressure-function solutions represent new information concerning the far-field behaviour of the flow. The practical motivation for the present study stems from computational fluid dynamics addressing large-eddy simulation (LES) and subgrid-scale (SGS) turbulence modelling. The asymptotic analysis of the fully developed region of the round jet is useful in examining the applicability of the results of the eddy-viscosity model to SGS turbulence. Furthermore, present results provide the far-field information, with which the conditions imposed on certain artificially introduced pseudo-boundaries in LES computations must be consistent.

Although the leading-order core-region and exterior-region solutions for the radial velocity match directly, the corresponding solutions for the other flow quantities do not. An examination of the leading-order *and* higher-order solutions for these two regions (but especially those for the core region) suggests the existence of the downstream intermediate region, formulated and analysed in §4. The leading-order intermediate-region solutions of all flow quantities match directly to all of the leading-order core-region solutions (in a near-field overlap domain) and also match directly to all of the leading-order exterior-region solutions (in a far-field overlap domain).

With the presentation of the pertinent solutions for the core, exterior, and intermediate regions, and with the determination of the core-region/intermediate-region matching and of the exterior-region/intermediate-region matching, the uniformly valid description of the structure of the self-similar turbulent axisymmetric jet is complete. The analytical predictions of the core-region distributions of the axial and radial velocities and the shear stress are compared in §6 with the experimental data of Wygnanski & Fiedler, with good results. Available experimental results, however, do not extend to the exterior region, as defined in this paper.

## 2. Equations of mean motion

Consider the steady flow of an axisymmetric/round fully developed turbulent jet of a homogeneous, incompressible fluid ($\tilde{\rho}$ = const.). Let $X = (\tilde{X}-\tilde{X}_0)/\tilde{B}_j$ and $R = \tilde{R}/\tilde{B}_j$ represent the axial and radial coordinates, with $\tilde{X}, \tilde{R} = 0$ denoting the origin of the jet, $\tilde{B}_j$ the initial jet radius, and $\tilde{X}_0$ the 'origin of similarity'. The mean velocity components in the axial and radial directions, respectively, are $U = \tilde{U}/\tilde{U}_j$ and $V = \tilde{V}/\tilde{U}_j$, with $\tilde{U}_j$ the reference jet-exit speed; the mean pressure is $P = (\tilde{P}-\tilde{P}_\infty)/\rho\tilde{U}_j^2$, with $\tilde{P}_\infty$ denoting the ambient pressure. The turbulent shear- and normal-stress components are

$$T = T_{XR} = T_{RX} = -\frac{\overline{\tilde{u}'\tilde{v}'}}{\tilde{U}_j^2}, \quad \text{and} \quad M = T_{XX} = -\frac{\overline{\tilde{u}'^2}}{\tilde{U}_j^2} \quad \text{and} \quad N = T_{RR} = -\frac{\overline{\tilde{v}'^2}}{\tilde{U}_j^2}.$$

In the foregoing, the tilde quantities are dimensional, the primes denote the fluctuating quantities, and the overbars denote time-averaging.

The continuity and momentum equations describing the mean flow are

$$\frac{\partial U}{\partial X}+\frac{1}{R}\frac{\partial (RV)}{\partial R} = 0: \quad U = \frac{1}{R}\frac{\partial \Psi}{\partial R}, \quad V = -\frac{1}{R}\frac{\partial \Psi}{\partial X}; \tag{2.1}$$

$$U\frac{\partial U}{\partial X}+V\frac{\partial U}{\partial R}+\frac{\partial P}{\partial X} = \frac{1}{R}\frac{\partial (RT)}{\partial R}+\frac{\partial M}{\partial X}, \tag{2.2a}$$

$$U\frac{\partial V}{\partial X}+V\frac{\partial V}{\partial R}+\frac{\partial P}{\partial R} = \frac{1}{R}\frac{\partial (RN)}{\partial R}+\frac{\partial T}{\partial X}. \tag{2.2b}$$

The far-field and centreline boundary conditions for (2.1) and (2.2) are

$$U, V, P, T, M, N \to 0 \quad \text{as} \quad R \to \infty; \tag{2.3a}$$

$$V, \frac{\partial U}{\partial R}, T \to 0, \quad U \to \text{finite} \quad \text{as} \quad R \to 0. \tag{2.3b}$$

The downstream analysis considered here does not address the initial conditions.

Integration of the continuity and momentum equations (2.1) and (2.2) with respect to $R$, over the domain of $R$, subject to the boundary conditions (2.3) yields

$$\frac{\mathrm{d}}{\mathrm{d}X}\int_0^\infty UR\,\mathrm{d}R = -(RV)\Big|_0^\infty = -(RV)_{,\infty} \equiv \tfrac{1}{2}E', \text{const.}; \tag{2.4}$$

$$\left.\begin{aligned} &\frac{\mathrm{d}}{\mathrm{d}X}\int_0^\infty [U^2+P-M]R\,\mathrm{d}R = -R[UV-T]\Big|_0^\infty = 0: \\ &\int_0^\infty [U^2+P-M]R\,\mathrm{d}R \equiv \frac{Z'}{2\pi}, \text{const.}, \end{aligned}\right\} \tag{2.5a}$$

$$\frac{\mathrm{d}}{\mathrm{d}X}\int_0^\infty [UV-T]R\,\mathrm{d}R = -R[V^2+P-N]\Big|_0^\infty + \int_0^\infty P\,\mathrm{d}R = \int_0^\infty P\,\mathrm{d}R. \tag{2.5b}$$

Here, $E'$ is the entrainment, and $Z'$ is the kinetic momentum.

## 3. The downstream core region

Attention is directed to the flow region far downstream of the nozzle exit, characterized by $x = \delta X$ and $r = R$, with $x, r \sim O(1)$, and with $\delta \ll 1$, such that $R/X = \delta(r/x) \sim O(\delta)$. The quantity $\delta$ is identified as a small parameter from a consideration of the experimental data for representing the centreline velocity as a function of the axial distance. In the present notation, to leading order of approximation, it is found that this representation is $U_{\mathfrak{c}} \approx (\delta X)^{-1}$, with $\delta \sim O(10^{-1})$ (see §6 for the details of this identification). The flow quantities for this downstream region are, in turn, scaled as

$$\Psi(X, R; \ldots) = \psi(x, r; \delta): \quad U = u, \quad V = \delta v, \tag{3.1a}$$

$$P(X, R; \ldots) = \delta p(x, r; \delta), \tag{3.1b}$$

$$T(X, R; \ldots) = \delta \tau(x, r; \delta), \quad M(X, R; \ldots) = \delta \mu(x, r; \delta), \quad N(X, R; \ldots) = \delta \nu(x, r; \delta). \tag{3.1c}$$

Thus, the differential equations of mean motion in this region are

$$\frac{\partial u}{\partial x} + \frac{1}{r}\frac{\partial (rv)}{\partial r} = 0: \quad u = \frac{1}{r}\frac{\partial \psi}{\partial r}, \quad v = -\frac{1}{r}\frac{\partial \psi}{\partial x}; \tag{3.2}$$

$$u\frac{\partial u}{\partial x} + v\frac{\partial u}{\partial r} + \delta\frac{\partial p}{\partial x} = \frac{1}{r}\frac{\partial (r\tau)}{\partial r} + \delta\frac{\partial \mu}{\partial x}, \tag{3.3a}$$

$$\delta\left(u\frac{\partial v}{\partial x} + v\frac{\partial v}{\partial r}\right) + \frac{\partial p}{\partial r} = \frac{1}{r}\frac{\partial (r\nu)}{\partial r} + \delta\frac{\partial \tau}{\partial x}. \tag{3.3b}$$

The centreline boundary conditions are, now,

$$v, \frac{\partial u}{\partial r}, \tau \to 0, \quad u \to \text{finite} \quad \text{as} \quad r \to 0. \tag{3.4}$$

In turn, (3.2)–(3.4) can be combined to give the following integral relations:

$$\frac{\partial}{\partial x}\int_0^r u\rho \, \mathrm{d}\rho = -rv, \tag{3.5a}$$

$$\frac{\partial}{\partial x}\int_0^r [u^2 + \delta(p - \mu)]\rho \, \mathrm{d}\rho = -r[uv - \tau], \tag{3.5b}$$

$$\delta\frac{\partial}{\partial x}\int_0^r [uv - \tau]\rho \, \mathrm{d}\rho = -r\left[\left(p - \frac{1}{r}\int_0^r p \, d\rho - \nu\right) + \delta v^2\right]. \tag{3.5c}$$

As $r \to \infty$, subject to verification of the far-field behaviour, it is taken that (3.5*b*) becomes

$$\left.\begin{aligned} &\frac{\mathrm{d}}{\mathrm{d}x}\int_0^\infty [u^2 + \delta(p - \mu)]\, r \, \mathrm{d}r = -(r[uv - \tau])_{,\infty} = 0: \\ &\int_0^\infty [u^2 + \delta(p - \mu)]\, r \, \mathrm{d}r \equiv \tfrac{1}{2}Z, \text{const.} \end{aligned}\right\} \tag{3.6}$$

Thus, (3.6) represents the core-region contribution to the (overall) axial-momentum integral relation of (2.5*a*).

For the self-similar formulation of this region, the independent and dependent variables are

$$\xi = x, \quad \eta = \frac{r}{x}; \tag{3.7}$$

$$\psi(x,r;\delta) = \xi F(\eta;\delta): \quad u = \xi^{-1}\frac{F'}{\eta}, \quad v = -\xi^{-1}\left(\frac{F}{\eta} - F'\right), \tag{3.8a}$$

$$p(x,r;\delta) = \xi^{-2}\Pi(\eta;\delta), \tag{3.8b}$$

$$\tau(x,r;\delta) = \xi^{-2}\Phi(\eta;\delta), \quad \mu(x,r;\delta) = \xi^{-2}J(\eta;\delta), \quad \nu(x,r;\delta) = \xi^{-2}K(\eta;\delta). \tag{3.8c}$$

Introduction of (3.7) and (3.8) into (3.2) and (3.3) produces

$$\left[\eta\Phi + F\frac{F'}{\eta} + \delta\{\eta^2(\Pi - J)\}\right]' = 0, \tag{3.9a}$$

$$\left[\eta(\Pi - K) + \delta\left\{\eta^2\Phi + F\left(\frac{F}{\eta} - F'\right)\right\}\right]' = \Pi. \tag{3.9b}$$

The primes in (3.8) and (3.9) denote differentiation with respect to $\eta$. The centreline boundary conditions are

$$F, F', \Phi \to 0, \quad \frac{F'}{\eta} \to \left(\frac{F'}{\eta}\right)_{,0} \quad \text{as} \quad \eta \to 0. \tag{3.10}$$

In this self-similar formulation, (3.6) becomes

$$\int_0^\infty \left[\left(\frac{F'}{\eta}\right)^2 + \delta(\Pi - J)\right]\eta\,\mathrm{d}\eta = \tfrac{1}{2}Z. \tag{3.11}$$

The introduction of the pressure-integral function, $\Lambda$, defined by

$$\Lambda = \int_0^\eta \Pi\,\mathrm{d}\eta', \quad \text{such that} \quad \Pi = \Lambda', \tag{3.12}$$

leads to the following self-similar boundary-value problem for the downstream core region of the turbulent round jet:

$$\eta\Phi + F\frac{F'}{\eta} + \delta\{\eta^2(\Lambda' - J)\} = 0, \tag{3.13a}$$

$$\eta(\Lambda' - K) - \Lambda + \delta\left\{\eta^2\Phi + F\left(\frac{F}{\eta} - F'\right)\right\} = 0; \tag{3.13b}$$

$$F, F', \Lambda, \Phi \to 0, \quad \frac{F'}{\eta} \to \left(\frac{F'}{\eta}\right)_{,0} \quad \text{as} \quad \eta \to 0; \tag{3.14}$$

$$\int_0^\infty \left[\left(\frac{F'}{\eta}\right)^2 + \delta(\Lambda' - J)\right]\eta\,\mathrm{d}\eta = \tfrac{1}{2}Z. \tag{3.15}$$

Note that (3.13$a$) and (3.13$b$) are the first integrals of (3.9$a$) and (3.9$b$), respectively, obtained through the employment of the centreline boundary conditions of (3.10) and (3.12).

A more detailed examination of this self-similar downstream region is facilitated with the introduction of the following asymptotic representations:

$$G(\eta;\delta) \sim G_0(\eta) + \delta G_1(\eta) + \ldots, \quad \text{with } G = F, \Lambda, \Phi, J, K. \tag{3.16}$$

Thus, the zeroth- and first-order boundary-value problems are

$$\eta\Phi_0+F_0\frac{F_0'}{\eta}=0, \tag{3.17a}$$

$$\eta(\Lambda_0'-K_0)-\Lambda_0=0: \quad \Pi_0=\Lambda_0', K_0=\eta\left(\frac{\Lambda_0}{\eta}\right)', \tag{3.17b}$$

$$F_0, F_0', \Lambda_0, \Phi_0 \to 0, \quad \frac{F_0'}{\eta}\to B_0 \quad \text{as} \quad \eta\to 0, \tag{3.17c}$$

$$\int_0^\infty \left(\frac{F_0'}{\eta}\right)^2 \eta\,\mathrm{d}\eta=\tfrac{1}{2}Z; \tag{3.17d}$$

$$\eta\Phi_1+F_0\frac{F_1'}{\eta}+\frac{F_0'}{\eta}F_1=-\eta^2(\Lambda_0'-J_0), \tag{3.18a}$$

$$\left.\begin{aligned}\eta(\Lambda_1'-K_1)-\Lambda_1&=-\left[\eta^2\Phi_0+F_0\left(\frac{F_0}{\eta}-F_0'\right)\right]=\eta\left(\frac{F_0^2}{\eta}\right)':\\ \Pi_1=\Lambda_1', \quad K_1&=\left[\eta\left(\frac{\Lambda_1}{\eta}\right)'-\left(\frac{F_0^2}{\eta}\right)'\right],\end{aligned}\right\} \tag{3.18b}$$

$$F_1, F_1', \Lambda_1, \Phi_1\to 0, \quad \frac{F_1'}{\eta}\to B_1 \quad \text{as} \quad \eta\to 0, \tag{3.18c}$$

$$\int_0^\infty \frac{F_0'}{\eta}\frac{F_1'}{\eta}\eta\,\mathrm{d}\eta=-\frac{1}{2}\int_0^\infty(\Lambda_0'-J_0)\,\eta\,\mathrm{d}\eta. \tag{3.18d}$$

To proceed, based on experiment and (constant-eddy-viscosity) theory (as reported by Hinze 1975, Schlichting 1979, and others), the zeroth-order approximation for the axial-velocity function is taken to be

$$\frac{F_0'}{\eta}=\frac{B_0}{(1+c^2\eta^2)^2}=B_0\frac{1}{(1+k)^2}, \tag{3.19a}$$

where $k=c^2\eta^2$. Introduction of (3.19*a*) into (3.17*d*) yields $(B_0/c)=(3Z)^{\frac{1}{2}}$. In what follows, it is taken that $B_0=1$, and, in turn, $c=(3Z)^{-\frac{1}{2}}$. The far-field and centreline behaviour for this function is

$$\frac{F_0'}{\eta}\to k^{-2}(1-2k^{-1}+\dots)\to 0 \quad \text{as} \quad k\to\infty, \tag{3.19b}$$

$$\frac{F_0'}{\eta}\to(1-2k+\dots)\to 1 \quad \text{as} \quad k\to 0. \tag{3.19c}$$

The corresponding approximation for the stream function is

$$F_0=\frac{B_0\eta^2}{2(1+c^2\eta^2)}=A_0\frac{k}{1+k}, \quad \text{with } A_0=\tfrac{3}{2}Z: \tag{3.20a}$$

$$F_0\to A_0(1-k^{-1}+\dots)\to A_0 \quad \text{as} \quad k\to\infty, \tag{3.20b}$$

$$F_0\to A_0k(1-k+\dots)\to 0 \quad \text{as} \quad k\to 0. \tag{3.20c}$$

From (3.19) and (3.20), the zeroth-order radial-velocity function is

$$\frac{F_0}{\eta}-F_0' = -\frac{B_0\,\eta(1-c^2\eta^2)}{2(1+c^2\eta^2)^2} = -\frac{1}{2c}\frac{k^{\frac{1}{2}}(1-k)}{(1+k)^2}: \tag{3.21a}$$

$$\frac{F_0}{\eta}-F_0' \to \frac{1}{2c}k^{-\frac{1}{2}}(1-3k^{-1}+\ldots)\to 0 \quad \text{as} \quad k\to\infty, \tag{3.21b}$$

$$\frac{F_0}{\eta}-F_0' \to -\frac{1}{2c}k^{\frac{1}{2}}(1-3k+\ldots)\to 0 \quad \text{as} \quad k\to 0. \tag{3.21c}$$

The leading-order approximation for the shear-stress function, in turn, is

$$\Phi_0 = -\frac{F_0}{\eta}\frac{F_0'}{\eta} = -\frac{B_0^2\,\eta}{2(1+c^2\eta^2)^3} = -\frac{1}{2c}\frac{k^{\frac{1}{2}}}{(1+k)^3}: \tag{3.22a}$$

$$\Phi_0 \to -\frac{1}{2c}k^{-\frac{5}{2}}(1-3k^{-1}+\ldots)\to 0 \quad \text{as} \quad k\to\infty, \tag{3.22b}$$

$$\Phi_0 \to -\frac{1}{2c}k^{\frac{1}{2}}(1-3k+\ldots)\to 0 \quad \text{as} \quad k\to 0. \tag{3.22c}$$

The experimental work of Wygnanski & Fiedler (1969) suggests the following approximations for $J_0$ and $K_0$:

$$J_0 = -\frac{a_0}{(1+c^2\eta^2)^2} = -a_0\frac{1}{(1+k)^2}, \quad \text{with } 0<a_0<1: \tag{3.23a}$$

$$J_0 \to -a_0 k^{-2}(1-2k^{-1}+\ldots)\to 0 \quad \text{as} \quad k\to\infty, \tag{3.23b}$$

$$J_0 \to -a_0(1-2k+\ldots)\to -a_0 \quad \text{as} \quad k\to 0; \tag{3.23c}$$

$$K_0 = -\frac{b_0}{(1+c^2\eta^2)^2} = -b_0\frac{1}{(1+k)^2}, \quad \text{with } 0<b_0<a_0<1: \tag{3.24a}$$

$$K_0 \to -b_0 k^{-2}(1-2k^{-1}+\ldots)\to 0 \quad \text{as} \quad k\to\infty, \tag{3.24b}$$

$$K_0 \to -b_0(1-2k+\ldots)\to -b_0 \quad \text{as} \quad k\to 0. \tag{3.24c}$$

The evaluation of $a_0$ and $b_0$ from experimental data is presented in §6. From (3.17*b*), it follows that

$$\Lambda_0 = \frac{b_0}{2c}k^{\frac{1}{2}}\left[\ln\left\{\frac{1+k}{k}\right\}-\frac{1}{1+k}\right]: \tag{3.25a}$$

$$\Lambda_0 \to \frac{b_0}{4c}k^{-\frac{3}{2}}(1-\tfrac{4}{3}k^{-1}+\ldots)\to 0 \quad \text{as} \quad k\to\infty, \tag{3.25b}$$

$$\Lambda_0 \to \frac{b_0}{2c}k^{\frac{1}{2}}[\ln(k^{-1})-1+2k-+\ldots]\to 0 \quad \text{as} \quad k\to 0. \tag{3.25c}$$

Thus, the leading-order approximation for the pressure function is

$$\Pi_0 = \Lambda_0' = \tfrac{1}{2}b_0\left[\ln\left\{\frac{1+k}{k}\right\}-\frac{3+k}{(1+k)^2}\right]: \tag{3.26a}$$

$$\Pi_0 \to -\tfrac{3}{4}b_0 k^{-2}(1-\tfrac{20}{9}k^{-1}+\ldots)\to 0 \quad \text{as} \quad k\to\infty, \tag{3.26b}$$

$$\Pi_0 \to \tfrac{1}{2}b_0[\ln(k^{-1})-3+6k+\ldots]\to\infty \quad \text{as} \quad k\to 0. \tag{3.26c}$$

The logarithmic blow-up of the 'models' for $\Lambda_0$ and $\Pi_0$ as $k \to 0$ is a consequence of the employment, in (3.17*b*), of the experimentally based 'model' for $K_0$, where $K_0 \to -b_0 < 0$. No further consideration is given to the centreline blow-up, as the emphasis of this paper is on the effect of the 'models' for the pressure and normal stresses on the far-field behaviour.

Now, the first-order approximation for the axial-velocity function is taken to be

$$\frac{F_1'}{\eta} = B_1 \frac{1}{(1+k)^2}, \quad \text{with } B_1 = -\tfrac{3}{4}(2a_0 - b_0) < 0: \tag{3.27a†}$$

$$\frac{F_1'}{\eta} \to B_1 k^{-2}(1 - 2k^{-1} + \ldots) \to 0 \quad \text{as} \quad k \to \infty, \tag{3.27b}$$

$$\frac{F_1'}{\eta} \to B_1(1 - 2k + \ldots) \to B_1 \quad \text{as} \quad k \to 0. \tag{3.27c}$$

The value of $B_1$ is determined from the first-order momentum-integral relation, (3.18*d*), with $B_0 = 1$. The corresponding stream function is

$$F_1 = A_1 \frac{k}{1+k}, \quad \text{with } A_1 = -\tfrac{9}{8}(2a_0 - b_0)Z < 0: \tag{3.28a}$$

$$F_1 \to A_1(1 - k^{-1} + \ldots) \to A_1 \quad \text{as} \quad k \to \infty, \tag{3.28b}$$

$$F_1 \to A_1 k(1 - k + \ldots) \to 0 \quad \text{as} \quad k \to 0. \tag{3.28c}$$

The first-order radial-velocity function is

$$\frac{F_1}{\eta} - F_1' = \frac{B_1}{2c} \frac{k^{\frac{1}{2}}(1-k)}{(1+k)^2}: \tag{3.29a}$$

$$\frac{F_1}{\eta} - F_1' \to \frac{B_1}{2c} k^{-\frac{1}{2}}(1 - 3k^{-1} + \ldots) \to 0 \quad \text{as} \quad k \to \infty, \tag{3.29b}$$

$$\frac{F_1}{\eta} - F_1' \to -\frac{B_1}{2c} k^{\frac{1}{2}}(1 - 3k + \ldots) \to 0 \quad \text{as} \quad k \to 0. \tag{3.29c}$$

The resulting first-order approximation for the shear-stress function is

$$\left.\begin{aligned} \Phi_1 &= -\left[\frac{F_0}{\eta}\frac{F_1'}{\eta} + \frac{F_0'}{\eta}\frac{F_1}{\eta} + \eta(\Pi_0 - J_0)\right] \\ &= -\frac{k^{\frac{1}{2}}}{c}\left\{\tfrac{1}{2}b_0\left[\ln\left\{\frac{1+k}{k}\right\} - \frac{1}{1+k}\right] + \frac{a_0 - b_0}{(1+k)^2} - \frac{\tfrac{3}{4}(2a_0 - b_0)}{(1+k)^3}\right\}: \end{aligned}\right\} \tag{3.30a}$$

$$\Phi_1 \to -\frac{k^{-\frac{3}{2}}}{4c}[(4a_0 - 3b_0) - \tfrac{1}{3}(42a_0 - 29b_0)k^{-1} + \ldots] \to 0 \quad \text{as} \quad k \to \infty, \tag{3.30b}$$

$$\Phi_1 \to -\frac{k^{\frac{1}{2}}}{2c}[b_0 \ln(k^{-1}) - \tfrac{1}{2}(2a_0 + 3b_0) + \tfrac{1}{2}(10a_0 + 3b_0)k + \ldots] \to 0 \quad \text{as} \quad k \to 0. \tag{3.30c}$$

† Thus, to this order of approximation, $F'/\eta \approx (F_0'/\eta) + \delta(F_1'/\eta) = (B_0 + \delta B_1)/(1+k)^2$, with $B_0 = 1$, $B_1 = -\tfrac{3}{4}(2a_0 - b_0)$, and the experimentally determined profile is maintained.

Here, the approximations for $J_1$ and $K_1$ are taken to be

$$J_1 = -a_1 \frac{1}{(1+k)^2}, \quad \text{with } a_1 = \text{const. (to be specified)}: \tag{3.31a†}$$

$$J_1 \to -a_1 k^{-2}(1-2k^{-1}+\ldots) \to 0 \quad \text{as} \quad k \to \infty, \tag{3.31b}$$

$$J_1 \to -a_1(1-2k+\ldots) \to -a_1 \quad \text{as} \quad k \to 0; \tag{3.31c}$$

$$K_1 = -b_1 \frac{1}{(1+k)^2}, \quad \text{with } b_1 = \text{const. (to be specified)}: \tag{3.32a†}$$

$$K_1 \to -b_1 k^{-2}(1-2k^{-1}+\ldots) \to 0 \quad \text{as} \quad k \to \infty, \tag{3.32b}$$

$$K_1 \to -b_1(1-2k+\ldots) \to -b_1 \quad \text{as} \quad k \to 0. \tag{3.32c}$$

From (3.18*b*), it is determined that, subject to the pertinent boundary conditions,

$$\Lambda_1 = -\frac{A_0}{4c}\frac{k^{\frac{1}{2}}(1-k)}{(1+k)^2} + \frac{b_1}{2c}\left[\ln\left\{\frac{1+k}{k}\right\} - \frac{1}{1+k}\right]. \tag{3.33}$$

In turn,

$$\Pi_1 = \Lambda_1' = -\tfrac{1}{4}A_0 \frac{1-6k+k^2}{(1+k)^3} + \tfrac{1}{2}b_1\left[\ln\left\{\frac{1+k}{k}\right\} - \frac{3+k}{(1+k)^2}\right]: \tag{3.34a}$$

$$\Pi_1 \to -\tfrac{1}{4}A_0 k^{-1}(1-9k^{-1}+\ldots) - \tfrac{3}{4}b_1 k^{-2}(1-+\ldots) \to 0 \quad \text{as} \quad k \to \infty, \tag{3.34b}$$

$$\Pi_1 \to -\tfrac{1}{4}A_0(1-9k+\ldots) + \tfrac{1}{2}b_1[\ln(k^{-1}) - 3 + 6k + \ldots] \to \infty \quad \text{as} \quad k \to 0. \tag{3.34c}$$

Higher-order solutions for the core-region flow quantities are not considered here. It is noted, however, that a preliminary study of the second-order boundary-value problems shows that the far-field behaviour of the velocity solutions of this order is such that the momentum-integral relation of (3.11) fails. This failure stems from the interaction of the higher-order core-region flow quantities with the leading-order quantities of the intermediate region analysed in §4, and with those of the exterior region, analysed in §5. This three-region interaction requires the consideration of the self-similar form of the momentum-integral relation of (2.5*a*), rather than (3.11).

From the preceding developments, it is now possible to determine the far-field behaviour of the solutions in the limit of $\eta \to \infty$, $\delta \to 0$, such that $\theta = \delta^{\frac{1}{2}}\eta \sim O(1)$. In this limit, $k = c^2\eta^2 = \frac{1}{3}Z\,\delta^{-1}\theta^2 \to \infty$; and

$$\begin{aligned}\Psi &\sim \xi[F_0+\delta F_1+\ldots] \\ &\to \xi[\tfrac{3}{2}Z - \delta\{\tfrac{9}{2}Z^2\theta^{-2} + \tfrac{9}{8}(2a_0-b_0)Z+\ldots\} + O(\delta^2)],\end{aligned} \tag{3.35a}$$

$$\begin{aligned}U &\sim \xi^{-1}\left[\frac{F_0'}{\eta} + \delta\frac{F_1'}{\eta}+\ldots\right] \\ &\to \delta^2\xi^{-1}[\{9Z^2\theta^{-4}+\ldots\} + O(\delta)],\end{aligned} \tag{3.35b}$$

$$\begin{aligned}V &\sim -\delta\xi^{-1}\left[\frac{F_0}{\eta} - F_0' + \delta\left(\frac{F_1}{\eta} - F_1'\right)+\ldots\right] \\ &\to -\delta^{\frac{3}{2}}\xi^{-1}[\tfrac{3}{2}Z\theta^{-1} - \delta\{\tfrac{27}{2}Z^2\theta^{-3} + \tfrac{9}{8}(2a_0-b_0)Z\theta^{-1}+\ldots\} + O(\delta^2)];\end{aligned} \tag{3.35c}$$

$$\begin{aligned}T &\sim \delta\xi^{-2}[\Phi_0+\delta\Phi_1+\ldots] \\ &\to -\delta^{\frac{7}{2}}\xi^{-2}[\{\tfrac{27}{2}Z^3\theta^{-5} + \tfrac{9}{4}(4a_0-3b_0)Z^2\theta^{-3}+\ldots\} + O(\delta)],\end{aligned} \tag{3.36a}$$

† To this order of approximation, $J \approx J_0 + \delta J_1 = -(a_0+\delta a_1)/(1+k)^2$, $K \approx K_0 + \delta K_1 = -(b_0+\delta b_1)/(1+k)^2$, and the experimentally determined profiles are maintained.

$$M \sim \delta\xi^{-2}[J_0+\delta J_1+\ldots]$$
$$\to -\delta^3\xi^{-2}[\{9a_0 Z^2\theta^{-4}+\ldots\}+O(\delta)], \quad (3.36b)$$
$$N \sim \delta\xi^{-2}[K_0+\delta K_1+\ldots]$$
$$\to -\delta^3\xi^{-2}[\{9b_0 Z^2\theta^{-4}+\ldots\}+O(\delta)]; \quad (3.36c)$$
$$P \sim \delta\xi^{-2}[\Pi_0+\delta\Pi_1+\ldots]$$
$$\to -\delta^3\xi^{-2}[\{\tfrac{27}{4}b_0 Z^2\theta^{-4}+\tfrac{9}{8}Z^2\theta^{-2}+\ldots\}+O(\delta)]. \quad (3.37)$$

## 4. The downstream intermediate region

The results of (3.35)–(3.37) indicate that, to ensure uniform validity, a region exterior to the downstream core region is required. For this region, designated here as the downstream intermediate region, the appropriate scalings of the original independent and dependent variables are

$$x_k = \delta X, \quad r_k = \delta^{\frac{1}{2}}R; \quad (4.1)$$

$$\Psi(X,R;\delta) = A_0 x_k+\delta\psi_k(x_k,r_k;\delta): \quad U=\delta^2 u_k, \quad V=-\delta^{\frac{3}{2}}\frac{A_0}{r_k}+\delta^{\frac{5}{2}}v_k, \quad (4.2a)$$

$$P(X,R;\delta) = \delta^3 p_k(x_k,r_k;\delta), \quad (4.2b)$$

$$\left.\begin{array}{c} T(X,R;\delta) = \delta^{\frac{7}{2}}\tau_k(x_k,r_k;\delta), \\ M(X,R;\delta) = \delta^3\mu_k(x_k,r_k;\delta), \quad N(X,R;\delta) = \delta^3\nu_k(x_k,r_k;\delta). \end{array}\right\} \quad (4.2c)$$

These variables are related to those of the core region through

$$x_k = x, \quad r_k = \delta^{\frac{1}{2}}r;$$
$$\psi = A_0 x_k+\delta\psi_k, \quad \text{with } A_0=\tfrac{3}{2}Z: \quad u=\delta^2 u_k, \quad v=\delta^{\frac{1}{2}}\left(-\frac{A_0}{r_k}+\delta v_k\right),$$
$$p=\delta^2 p_k, \quad \tau=\delta^{\frac{5}{2}}\tau_k, \quad \mu=\delta^2\mu_k, \quad \nu=\delta^2\nu_k. \quad (4.3)$$

Introduction of (4.1) and (4.2) into (2.1) and (2.2) produces

$$\frac{\partial u_k}{\partial x_k}+\frac{1}{r_k}\frac{\partial(r_k v_k)}{\partial r_k}=0: \quad u_k=\frac{1}{r_k}\frac{\partial\psi_k}{\partial r_k}, \quad v_k=-\frac{1}{r_k}\frac{\partial\psi_k}{\partial x_k}; \quad (4.4)$$

$$-\frac{A_0}{r_k}\frac{\partial u_k}{\partial r_k}+\delta\left(u_k\frac{\partial u_k}{\partial x_k}+v_k\frac{\partial u_k}{\partial r_k}\right)+\frac{\partial p_k}{\partial x_k}=\frac{1}{r_k}\frac{\partial(r_k\tau_k)}{\partial r_k}+\frac{\partial\mu_k}{\partial x_k}, \quad (4.5a)$$

$$-\frac{A_0^2}{r_k^3}-\delta A_0\frac{\partial}{\partial r_k}\left(\frac{v_k}{r_k}\right)+\delta^2\left(u_k\frac{\partial v_k}{\partial x_k}+v_k\frac{\partial v_k}{\partial r_k}\right)+\frac{\partial p_k}{\partial r_k}=\frac{1}{r_k}\frac{\partial(r_k\nu_k)}{\partial r_k}+\delta\frac{\partial\tau_k}{\partial x_k}. \quad (4.5b)$$

It is seen that these scalings for the variables yield a region in which there is, to leading-order of approximation, a convection–pressure-gradient–shear-stress–normal-stress balance in the axial-momentum equation, (4.5*a*), and a convection–pressure-gradient–normal-stress balance in the radial-momentum equation, (4.5*b*).

A self-similar formulation of this intermediate region is sought through the introduction of the following variables:

$$\xi = x_k, \quad \theta = r_k/x_k; \quad (4.6)$$

$$\psi_k(x_k,r_k;\delta)=\xi F_k(\theta;\delta): \quad u_k=\xi^{-1}\frac{F_k'}{\theta}, \quad v_k=-\xi^{-1}\left(\frac{F_k}{\theta}-F_k'\right), \quad (4.7a)$$

$$p_k(x_k,r_k;\delta)=\xi^{-2}\Pi_k(\theta;\delta)\equiv\xi^{-2}\Lambda_k'(\theta;\delta), \quad (4.7b)$$

$$\tau_k(x_k,r_k;\delta)=\xi^{-2}\Phi_k(\theta;\delta), \quad \mu_k(x_k,r_k;\delta)=\xi^{-2}J_k(\theta;\delta), \quad \nu_k(x_k,r_k;\delta)=\xi^{-2}K_k(\theta;\delta). \quad (4.7c)$$

The independent variables of the intermediate region are related to those of the core region by

$$\xi = x_k = x, \quad \theta = r_k/x_k = \delta^{\frac{1}{2}} r/x = \delta^{\frac{1}{2}}\eta. \tag{4.8}$$

The resulting self-similar axial- and radial-momentum equations are

$$\left\{\theta\left[\Phi_k + \frac{A_0}{\theta}\frac{F'_k}{\theta}\right] + \theta^2(A'_k - J_k)\right\} + \delta\left\{F_k \frac{F'_k}{\theta}\right\} = 0, \tag{4.9a}$$

$$\left\{\theta\left[A'_k - \frac{A_k}{\theta} - K_k + \frac{A_0^2}{\theta^2}\right]\right\} + \delta\left\{\theta^2\Phi_k + A_0\left(2\frac{F_k}{\theta} - F'_k\right)\right\} + \delta^2\left\{F_k\left(\frac{F_k}{\theta} - F'_k\right)\right\} = 0. \tag{4.9b}$$

Again, it is appropriate to introduce asymptotic representations for the dependent variables, i.e.,

$$G_k(\theta;\delta) \sim G_{k0}(\theta) + \ldots, \quad \text{with } G_k = F_k, A_k\, \Phi_k, J_k, K_k. \tag{4.10}$$

Thus, the zeroth-order equations for the intermediate region are

$$\Phi_{k0} + \frac{A_0}{\theta}\frac{F'_{k0}}{\theta} + \theta(A'_{k0} - J_{k0}) = 0, \tag{4.11a}$$

$$A'_{k0} - \frac{A_{k0}}{\theta} - K_{k0} + \frac{A_0^2}{\theta^2} = 0. \tag{4.11b}$$

The solutions of (4.11) that match to those of the (far-field) core region of §3 – and that match to those of the *anticipated* (near-field) exterior region of §5 – are

$$F_{k0} = \tfrac{1}{4}A_0\theta^2 + A_1 - 2A_0^2\theta^{-2}: \tag{4.12a}$$

$$\frac{F'_{k0}}{\theta} = \tfrac{1}{2}A_0 + 4A_0^2\theta^{-4}, \quad \frac{F_{k0}}{\theta} - F'_{k0} = -\{\tfrac{1}{4}A_0\theta - A_1\theta^{-1} + 6A_0^2\theta^{-3}\}; \tag{4.12b, c}$$

$$\Phi_{k0} = -\{\tfrac{1}{2}A_0\theta^{-1} + (4a_0 - 3b_0)A_0^2\theta^{-3} + 4A_0^3\theta^{-5}\}, \tag{4.13a}$$

$$J_{k0} = -\{\mu_0\theta^{-2} + 4a_0A_0^2\theta^{-4}\}, \quad K_{k0} = -\{\nu_0\theta^{-2} + 4b_0A_0^2\theta^{-4}\}, \quad \text{with } 2\mu_0 - \nu_0 = A_0^2; \tag{4.13b, c}$$

$$\Pi_{k0} = -\{\mu_0\theta^{-2} + 3b_0A_0^2\theta^{-4}\}. \tag{4.14}$$

Recall that $A_0 = \frac{3}{2}Z$, $A_1 = -\frac{9}{8}(2a_0 - b_0)Z$, .... Higher-order solutions for this intermediate region are not pursued here.

In the limit of $\theta \to \infty$, $\delta \to 0$, such that $\zeta = \delta^{\frac{1}{2}}\theta \sim O(1)$, the variables of the intermediate region have the following behaviours:

$$\Psi \sim \xi[A_0 + \delta F_{k0} + \ldots] \to \xi[A_0(1 + \tfrac{1}{4}\zeta^2) + O(\delta)], \tag{4.15a}$$

$$U \sim \delta^2\xi^{-1}\left[\frac{F'_{k0}}{\theta} + \ldots\right] \to \delta^2\xi^{-1}[\tfrac{1}{2}A_0 + O(\delta)], \tag{4.15b}$$

$$V \sim -\delta^{\frac{3}{2}}\xi^{-1}\left[A_0\theta^{-1} - \delta\left(F'_{k0} - \frac{F_{k0}}{\theta}\right) + \ldots\right] \to -\delta^2\xi^{-1}[A_0\zeta^{-1}(1 - \tfrac{1}{4}\zeta^2) + O(\delta)]; \tag{4.15c}$$

$$T \sim \delta^{\frac{7}{2}}\xi^{-2}[\Phi_{k0} + \ldots] \to -\delta^4\xi^{-2}[\tfrac{1}{2}A_0^2\zeta^{-1} + O(\delta)], \tag{4.16a}$$

$$M \sim \delta^3\xi^{-2}[J_{k0} + \ldots] \to -\delta^4\xi^{-2}[\mu_0\zeta^{-2} + O(\delta)], \tag{4.16b}$$

$$N \sim \delta^3\xi^{-2}[K_{k0} + \ldots] \to -\delta^4\xi^{-2}[\nu_0\zeta^{-2} + O(\delta)]; \tag{4.16c}$$

$$P \sim \delta^3\xi^{-2}[\Pi_{k0} + \ldots] \to -\delta^4\xi^{-2}[\mu_0\zeta^{-2} + O(\delta)], \tag{4.17}$$

## 5. The downstream exterior region

The uniformly valid characterization of the far-field development of the turbulent round jet is completed through the introduction of the downstream exterior region, wherein the axial and radial lengthscales are equal, i.e.

$$x_s = \delta X, \quad r_s = \delta R; \tag{5.1}$$

and the appropriate scalings of the flow quantities are

$$\Psi(X,R;\delta) = \psi_s(x_s, r_s;\delta): \quad U = \delta^2 u_s, \quad V = \delta^2 v_s, \tag{5.2a}$$

$$P(X,R;\delta) = \delta^4 p_s(x_s, r_s;\delta), \tag{5.2b}$$

$$T(X,R;\delta) = \delta^4 \tau_s(x_s, r_s;\delta), \quad M(X,R;\delta) = \delta^4 \mu_s(x_s, r_s;\delta), \quad N(X,R;\delta) = \delta^4 \nu_s(x_s, r_s;\delta). \tag{5.2c}$$

In this region, the vorticity is

$$\Omega(X,R;\delta) = \frac{\partial V}{\partial X} - \frac{\partial U}{\partial R} = \delta^3 \omega_s(x_s, r_s;\delta) = \delta^3\left(\frac{\partial v_s}{\partial x_s} - \frac{\partial u_s}{\partial r_s}\right). \tag{5.3}$$

In terms of these exterior-region variables, the equations of motion are

$$\frac{\partial u_s}{\partial x_s} + \frac{1}{r_s}\frac{\partial (r_s v_s)}{\partial r_s} = 0: \quad u_s = \frac{1}{r_s}\frac{\partial \psi_s}{\partial r_s}, \quad v_s = -\frac{1}{r_s}\frac{\partial \psi_s}{\partial x_s}; \tag{5.4}$$

$$u_s \frac{\partial u_s}{\partial x_s} + v_s \frac{\partial u_s}{\partial r_s} + \frac{\partial p_s}{\partial x_s} = \frac{1}{r_s}\frac{\partial (r_s \tau_s)}{\partial r_s} + \frac{\partial \mu_s}{\partial x_s}, \tag{5.5a}$$

$$u_s \frac{\partial v_s}{\partial x_s} + v_s \frac{\partial v_s}{\partial r_s} + \frac{\partial p_s}{\partial r_s} = \frac{1}{r_s}\frac{\partial (r_s \nu_s)}{\partial r_s} + \frac{\partial \tau_s}{\partial x_s}. \tag{5.5b}$$

Taking this exterior region to be an irrotational one, (5.3) becomes

$$\frac{\partial v_s}{\partial x_s} - \frac{\partial u_s}{\partial r_s} = -\left[\frac{\partial^2 \psi_s}{\partial x_s^2} + r_s \frac{\partial}{\partial r_s}\left(\frac{1}{r_s}\frac{\partial \psi_s}{\partial r_s}\right)\right] = 0. \tag{5.6}$$

The boundary conditions for these equations are

$$u_s, v_s, p_s, \tau_s, \mu_s, \nu_s \to 0 \quad \text{as} \quad r_s \to \infty. \tag{5.7}$$

Again, a self-similar formulation is sought for this region in terms of the following variables:

$$\xi = x_s, \quad \zeta = r_s/x_s; \tag{5.8}$$

$$\left.\begin{aligned} &\psi_s(x_s, r_s;\delta) = \xi F_s(\zeta;\delta): \\ &u_s = \xi^{-1}\frac{F_s'}{\zeta}, \quad v_s = -\xi^{-1}\left(\frac{F_s}{\zeta} - F_s'\right), \\ &\omega_s = -\xi^{-2}\left[\frac{1+\zeta^2}{\zeta}\left(F_s' - \frac{\zeta}{1+\zeta^2}F_s\right)\right]', \end{aligned}\right\} \tag{5.9a}$$

$$p_s(x_s, r_s;\delta) = \xi^{-2}\Pi_s(\zeta;\delta) \equiv \xi^{-2}\Lambda_s'(\zeta;\delta), \tag{5.9b}$$

$$\tau_s(x_s, r_s;\delta) = \xi^{-2}\Phi_s(\zeta;\delta), \quad \mu_s(x_s, r_s;\delta) = \xi^{-2}J_s(\zeta;\delta), \quad \nu_s(x_s, r_s;\delta) = \xi^{-2}K_s(\zeta;\delta). \tag{5.9c}$$

Note that $\zeta = r_s/x_s = R/X = \delta^{\frac{1}{2}}\theta = \delta\eta$.

In turn, (5.5) and (5.6), subject to (5.7), can be written as

$$\left\{\Phi_s+\frac{F'_s}{\zeta}\left(\frac{F_s}{\zeta}-F'_s\right)\right\}+\zeta\left\{(\Lambda'_s-J_s)+\left(\frac{F'_s}{\zeta}\right)^2\right\}=0, \tag{5.10a}$$

$$\left\{\Lambda'_s-\frac{\Lambda_s}{\zeta}-K_s+\left(\frac{F_s}{\zeta}-F'_s\right)^2\right\}+\zeta\left\{\Phi_s+\frac{F'_s}{\zeta}\left(\frac{F_s}{\zeta}-F'_s\right)\right\}=0; \tag{5.10b}$$

$$\left[\frac{1+\zeta^2}{\zeta}\left(F'_s-\frac{\zeta}{1+\zeta^2}F_s\right)\right]'=0. \tag{5.11}$$

An asymptotic analysis of this region, in terms of an expansion of the form

$$G_s(\zeta;\delta)\sim G_{s0}(\zeta)+\dots,\quad \text{with } G_s=F_s,\Lambda_s,\Phi_s,J_s,K_s, \tag{5.12}$$

from a consideration of (5.10) and (5.11), leads to

$$F_{s0}=\tfrac{1}{2}A_0[(1+\zeta^2)^{\frac{1}{2}}+1]: \tag{5.13a}$$

$$\frac{F'_{s0}}{\zeta}=\tfrac{1}{2}A_0(1+\zeta^2)^{-\frac{1}{2}},\quad \frac{F_{s0}}{\zeta}-F'_{s0}=\tfrac{1}{2}A_0\,\zeta^{-1}[1+(1+\zeta^2)^{-\frac{1}{2}}]; \tag{5.13b}$$

$$\Phi_{s0}=-\frac{F'_{s0}}{\zeta}\left(\frac{F_{s0}}{\zeta}-F'_{s0}\right)=-\tfrac{1}{4}A_0^2\,\zeta^{-1}(1+\zeta^2)^{-\frac{1}{2}}[1+(1+\zeta^2)^{-\frac{1}{2}}], \tag{5.14a}$$

$$\Lambda'_{s0}-J_{s0}=-\left(\frac{F'_{s0}}{\zeta}\right)^2=-\tfrac{1}{4}A_0^2(1+\zeta^2)^{-1}, \tag{5.14b}$$

$$\Lambda'_{s0}-\frac{\Lambda_{s0}}{\zeta}-K_{s0}=-\left(\frac{F_{s0}}{\zeta}-F'_{s0}\right)^2=-\tfrac{1}{4}A_0^2\,\zeta^{-2}[1+(1+\zeta^2)^{-\frac{1}{2}}]^2. \tag{5.14c}$$

The results for the velocity functions of (5.13) are consistent with those reported by Landau & Lifshitz (1959). The results of (5.14) represent new information concerning the behaviour of the stress functions in the far-field. Higher-order solutions for the exterior region are not pursued here.

The far-field ($\zeta\to\infty$) behaviour of these zeroth-order functions is

$$F_{s0}\sim\tfrac{1}{2}A_0\,\zeta(1+\zeta^{-1}+\dots)\to\infty: \tag{5.15a}$$

$$\frac{F'_{s0}}{\zeta}\sim\tfrac{1}{2}A_0\,\zeta^{-1}(1-\tfrac{1}{2}\zeta^{-2}+\dots)\to 0, \tag{5.15b}$$

$$\frac{F_{s0}}{\zeta}-F'_{s0}\sim\tfrac{1}{2}A_0\,\zeta^{-1}(1+\zeta^{-1}+\dots)\to 0; \tag{5.15c}$$

$$\Phi_{s0}\sim-\tfrac{1}{4}A_0^2\,\zeta^{-2}(1+\dots)\to 0, \tag{5.16a}$$

$$\Lambda'_{s0}-J_{s0}\sim-\tfrac{1}{4}A_0^2\,\zeta^{-2}(1+\dots)\to 0, \tag{5.16b}$$

$$\Lambda'_{s0}-\frac{\Lambda_{s0}}{\zeta}-K_{s0}\sim-\tfrac{1}{4}A_0^2\,\zeta^{-2}(1+\dots)\to 0. \tag{5.16c}$$

It is noted that the behaviour of the pressure and normal-stress functions is

$$\Pi_{s0}=\Lambda'_{s0}\sim-\pi_0\,\zeta^{-2}(1+\dots),\quad J_{s0}\sim-\alpha_0\,\zeta^{-2}(1+\dots),\quad K_{s0}\sim-\beta_0\,\zeta^{-2}(1+\dots),$$

if

$$(\pi_0-\alpha_0),(2\pi_0-\beta_0)=\tfrac{1}{4}A_0^2,\ \text{i.e.}\quad(\pi_0+\alpha_0-\beta_0)=0. \tag{5.17}$$

The near-field ($\zeta \to 0$) behaviour of these functions is

$$F_{s0} \sim A_0(1+\tfrac{1}{4}\zeta^2+\ldots) \to A_0: \tag{5.18a}$$

$$\frac{F'_{s0}}{\zeta} \sim \tfrac{1}{2}A_0(1-\tfrac{1}{2}\zeta^2+\ldots) \to \tfrac{1}{2}A_0, \tag{5.18b}$$

$$\frac{F_{s0}}{\zeta} - F'_{s0} \sim A_0\zeta^{-1}(1-\tfrac{1}{4}\zeta^2+\ldots) \to \infty; \tag{5.18c}$$

$$\Phi_{s0} \sim -\tfrac{1}{2}A_0^2\zeta^{-1}(1-\tfrac{3}{4}\zeta^2+\ldots) \to -\infty, \tag{5.19a}$$

$$A'_{s0} - J_{s0} \sim -\tfrac{1}{4}A_0^2(1-\zeta^2+\ldots) \to -\tfrac{1}{4}A_0^2, \tag{5.19b}$$

$$A'_{s0} - \frac{A_{s0}}{\zeta} - K_{s0} \sim -A_0^2\zeta^{-2}(1-\tfrac{1}{2}\zeta^2+\ldots) \to -\infty. \tag{5.19c}$$

The behaviour of the pressure and normal-stress functions is

$$\Pi_{s0} = A'_{s0} \sim -\pi_0\zeta^{-2}(1+\ldots), \quad J_{s0} \sim -\mu_0\zeta^{-2}(1+\ldots), \quad K_{s0} \sim -\nu_0\zeta^{-2}(1+\ldots),$$

if

$$\pi_0 = \mu_0 \quad \text{and} \quad 2\mu_0 - \nu_0 = A_0^2. \tag{5.20}$$

It is seen that these functions (i) satisfy the boundary conditions at infinity, and (ii) match to the far-field behaviour of the intermediate-region functions.

## 6. Results and discussion

The experimental data for the centreline velocity as a function of axial distance are expressed, in the present notation, as

$$U_{\mathfrak{c}} = \frac{\tilde{U}_c}{\tilde{U}_j} \approx \frac{C}{(\tilde{X}-\tilde{X}_0)/2\tilde{B}_j} = \frac{2C}{X}, \quad \text{with } C = \text{const. (determined experimentally)}, \tag{6.1}$$

i.e. the centreline velocity is inversely proportional to the axial distance in the self-similar downstream zone. Hinze & Van der Hegge Zijnen (1949, hereinafter referred to as H–VdHZ), found $C \approx 5.9$, $(2C)^{-1} \approx 0.085$ for $20 < X < 100$; Wygnanski & Fiedler (1969, referred to as W–F), found $C \approx 5.4$, $(2C)^{-1} \approx 0.093$ for $50 < X < 180$. In the self-similar analysis of §3, it is found that the centreline velocity is

$$U_{\mathfrak{c}} \sim \xi^{-1}[B_0 + \delta B_1 + \ldots], \quad \text{with } \xi = \delta X, \quad B_0 = 1, \quad B_1 = -\tfrac{3}{4}(2a_0 - b_0), \quad \ldots. \tag{6.2}$$

From the W–F data, $\delta B_1 \approx -0.079$ (as is shown later in this section). A comparison of (6.1) and (6.2) indicates that, if terms of $O(\delta^2)$ are neglected,

$$\left.\begin{aligned} 2C \approx \delta^{-1}[1+(\delta B_1)] \quad \text{and/or} \quad \delta \approx (2C)^{-1}[1+(\delta B_1)]: \\ \delta \approx 0.086 \text{ for } (2C)^{-1} \approx 0.093, \quad \delta B_1 \approx -0.079. \end{aligned}\right\} \tag{6.3}$$

For the purpose of consistency only, hereinafter W–F is employed as the basis for comparison.

The axial-velocity-distribution data are (most often) presented as

$$U^* = \frac{U}{U_{\mathfrak{c}}} \approx \frac{1}{(1+L^2\zeta^2)^2} \equiv U^*_{\text{CORE}}(\zeta; L),$$

with

$$\zeta = R/X, \quad L^2 = \text{const. (determined experimentally)}. \tag{6.4}$$

The measurements of H–VdHZ give $L^2 \approx 63.8$; W–F find $L^2 \approx 57.8$. When terms of $O(\delta^2)$ are neglected, the core-region analysis of §3 shows that

$$U^* = \frac{U}{U_{\mathfrak{c}}} \approx \frac{1}{(1+c^2\eta^2)^2}, \quad \text{with } \eta = \delta^{-1}R/X, \quad c = (3Z)^{-\frac{1}{2}}. \tag{6.5}$$

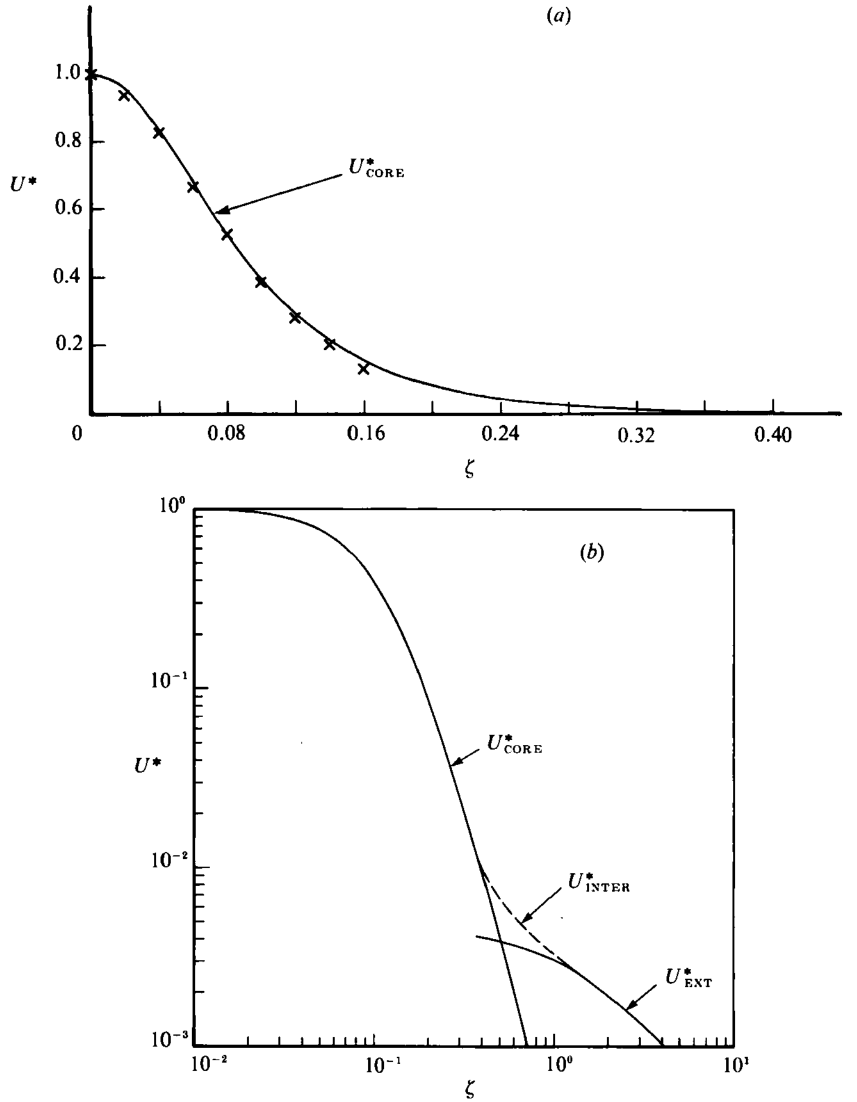


FIGURE 1. (*a*). Comparison with mean-velocity data of Wygnanski & Fiedler (1969) (×). (*b*) Core-, intermediate-, and exterior-region mean-velocity prediction.

A comparison of (6.4) and (6.5) yields

$$\left.\begin{array}{c} L^2 \approx (3Z\delta^2)^{-1} \quad \text{and/or} \quad Z \approx (3\delta^2L^2)^{-1}: \\ Z \approx 0.78, \quad c = (3Z)^{-\frac{1}{2}} \approx 0.65, \quad A_0 = \frac{3}{2}Z \approx 1.2 \quad \text{for } \delta \approx 0.086, \quad L^2 \approx 57.8. \end{array}\right\} \tag{6.6}$$

The far-field axial-velocity distribution determined by the zeroth-order exterior-region analysis of §5, with $\frac{1}{2}\delta^2 A_0 = (4L^2)^{-1}$, is

$$U^* = \frac{U}{U_{\mathfrak{c}}} \approx \frac{(4L^2)^{-1}}{(1+\zeta^2)^{\frac{3}{2}}} \equiv U^*_{\text{EXT}}(\zeta;L), \quad \text{with} \quad (4L^2)^{-1} \approx 0.00433 \quad \text{for} \quad L^2 \approx 57.8. \tag{6.7}$$

In figure 1(*a*), $U^*_{\text{CORE}}(\zeta;L)$, given by (6.4), is compared with the data of W–F. Not surprisingly, this representation compares well with the data. Figure 1(*b*) shows $U^*_{\text{CORE}}(\zeta;L)$ and $U^*_{\text{EXT}}(\zeta;L)$ of (6.4) and (6.7), respectively, as well as $U^*_{\text{INTER}}(\zeta;L)$, the intermediate-region representation. Since the data of W–F (and others) do not

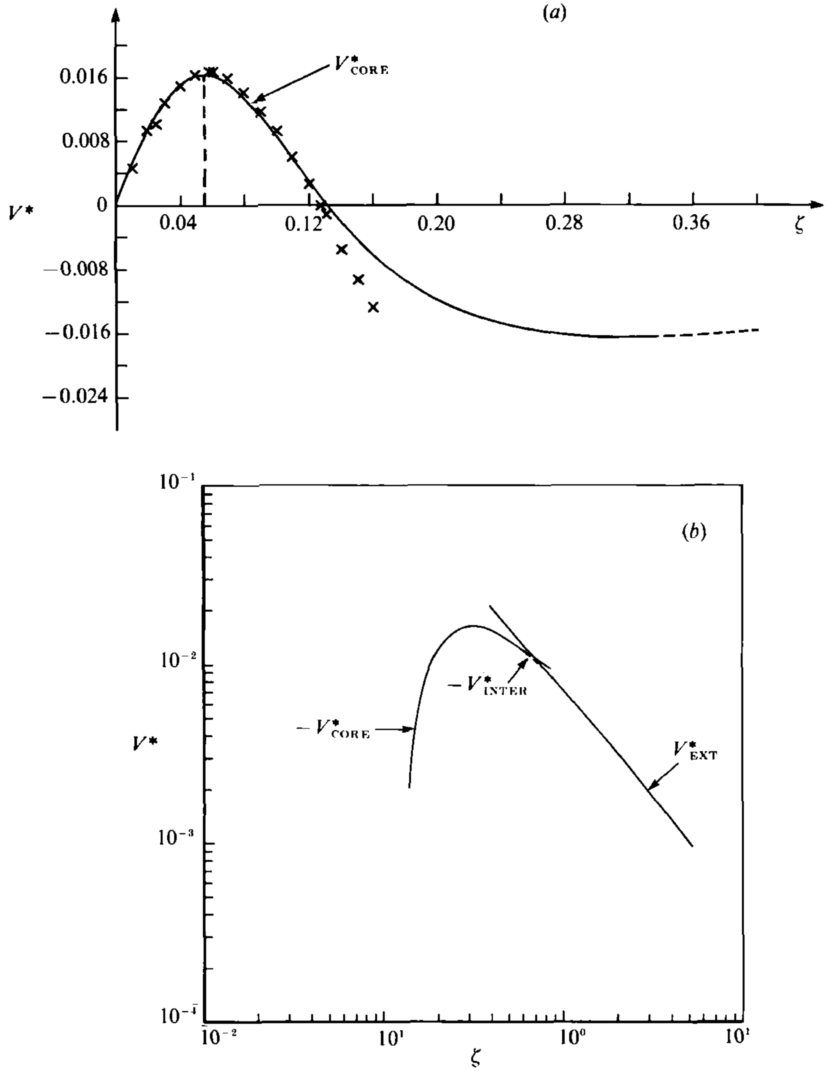


FIGURE 2. (a) Comparison of radial-velocity distribution across the jet, with W–F (×). (b) Core-, intermediate-, and exterior-region radial-velocity results.

extend to the exterior region, as defined in this paper, it is not possible to make a far-field comparison.

When terms of $O(\delta^2)$ are neglected, the core-region radial-velocity distribution can be expressed as

$$V^* = \frac{V}{U_{\mathfrak{c}}} \approx \frac{\zeta(1-L^2\zeta^2)}{2(1+L^2\zeta^2)^2} \equiv V^*_{\text{CORE}}(\zeta;L). \tag{6.8}$$

The zeroth-order exterior-region radial-velocity distribution is given by

$$V^* = \frac{V}{U_{\mathfrak{c}}} \approx -\frac{(4L^2)^{-1}\,[(1+\zeta^2)^{\frac{1}{2}}+1]}{\zeta(1+\zeta^2)^{\frac{1}{2}}} \equiv V^*_{\text{EXT}}(\zeta;L). \tag{6.9}$$

Figure 2(a) compares $V^*_{\text{CORE}}(\zeta;L)$, of (6.8), with the data of W–F. Again, the comparison is good. The solutions $V^*_{\text{CORE}}(\zeta;L)$, $V^*_{\text{EXT}}(\zeta;L)$, and $V^*_{\text{INTER}}(\zeta;L)$ are shown in figure 2(b).

Since, for the core region,

$$T = -\frac{\overline{\tilde{u}'\tilde{v}'}}{\tilde{U}_j^2} = -\overline{u'v'} = \delta\tau = \delta\xi^{-2}\Phi,$$

the pertinent zeroth-order representation for the shear-stress distribution is

$$\Phi^* = \frac{\overline{u'v'}}{U_{\mathrm{c}}^2} \approx \frac{\zeta}{2(1+L^2\zeta^2)^3} \equiv \Phi^*_{\mathrm{CORE}}(\zeta;L). \tag{6.10}$$

This is essentially the relation for the shear-stress distribution employed by Hinze (1975). For the exterior region,

$$T = -\frac{\overline{\tilde{u}'\tilde{v}'}}{\tilde{U}_j^2} = -\overline{u'v'} = \delta^4\tau_s = \delta^4\xi^{-2}\Phi_s,$$

and the corresponding zeroth-order shear-stress distribution is

$$\left.\begin{aligned} \Phi^* &= \frac{\overline{u'v'}}{U_{\mathrm{c}}^2} \approx \frac{(4L^2)^{-2}\,[(1+\zeta^2)^{\frac{1}{2}}+1]}{\zeta(1+\zeta^2)} \equiv \Phi^*_{\mathrm{EXT}}(\zeta;L),\\ \text{with}\quad & (4L^2)^{-2} \approx 0.0000187 \quad \text{for} \quad L^2 \approx 57.8. \end{aligned}\right\} \tag{6.11}$$

In figure 3(*a*), $\Phi^*_{\mathrm{CORE}}(\zeta;L)$, of (6.10), is compared with the data of W–F, with good results. Figure 3(*b*) displays the solutions $\Phi^*_{\mathrm{CORE}}(\zeta;L)$, $\Phi^*_{\mathrm{EXT}}(\zeta;L)$, and $\Phi^*_{\mathrm{INTER}}(\zeta;L)$.

For the core region, the normal-stress components are

$$M = -\frac{\overline{\tilde{u}'^2}}{\tilde{U}_j^2} = -\overline{u'^2} = \delta\mu = \delta\xi^{-2}J,$$

$$N = -\frac{\overline{\tilde{v}'^2}}{\tilde{U}_j^2} = -\overline{v'^2} = \delta\nu = \delta\xi^{-2}K,$$

where, at the very least, the zeroth-order approximations/models, $J_0$ and $K_0$, employed in the analysis presented in §3, require the specification of the centreline values, $a_0$ and $b_0$, respectively. The data of W–F, in conjunction with these zeroth-order models, lead to the normal-stress distributions

$$\frac{(\overline{u'^2})^{\frac{1}{2}}}{U_{\mathrm{c}}} \approx \frac{(\delta a_0)^{\frac{1}{2}}}{1+L^2\zeta^2}, \quad \frac{(\overline{v'^2})^{\frac{1}{2}}}{U_{\mathrm{c}}} \approx \frac{(\delta b_0)^{\frac{1}{2}}}{1+L^2\zeta^2}, \quad \text{with} \quad (\delta a_0)^{\frac{1}{2}} \approx 0.29, \quad (\delta b_0)^{\frac{1}{2}} \approx 0.25. \tag{6.12}$$

From (6.12), $\delta a_0 \approx 0.084$, $\delta b_0 \approx 0.063$: $a_0 \approx 0.98$, $b_0 \approx 0.73$ for $\delta \approx 0.086$, and, in turn,

$$\begin{aligned} \delta B_1 &\approx -0.079: \quad B_1 \approx -0.92 \quad \text{for} \quad \delta \approx 0.086,\\ \delta A_1 = A_0(\delta B_1) &\approx -0.095: \quad A_1 \approx -1.1 \quad \text{for} \quad \delta \approx 0.086, \quad Z \approx 0.78. \end{aligned} \tag{6.13}$$

The evaluation of $\delta B_1$ follows directly from the normal-stress data/model comparison, without the specification of $\delta$. Thus, it is consistent to employ $\delta B_1 \approx -0.079$ to evaluate $\delta$, as is done in (6.3).

The research reported herein was supported in part by the United States Air Force Office of Scientific Research under Contract No. F49620-88-C-0040 (Major James M. Crowley, Project Monitor).

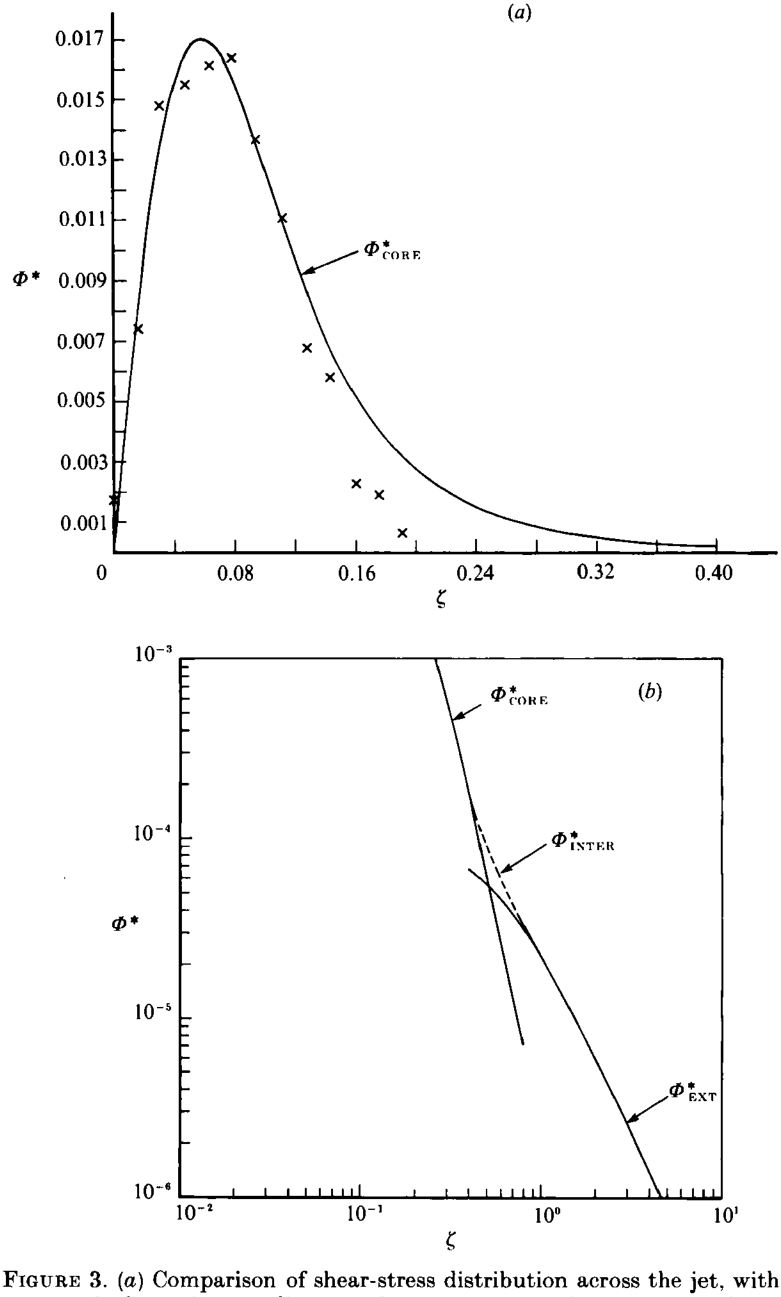


FIGURE 3. (a) Comparison of shear-stress distribution across the jet, with W–F (×). (b) Core-, intermediate-, and exterior-region shear-stress predictions.

## REFERENCES


ABRAMOVICH, G. N. 1963 *The Theory of Turbulent Jets* (transl. by Scripta Technica; techn. ed. L. H. Schindel). M. I. T. Press.

HINZE, J. O. 1975 *Turbulence* (2nd edn). McGraw-Hill.

HINZE, J. O. & VAN DER HEGGE ZIJNEN, B. G. 1949 Transfer of heat and matter in the turbulent mixing zone of an axially symmetric jet. *Appl. Sci. Res.* **1A**, 435 (referred to herein as H–VdHZ).

LANDAU, L. D. & LIFSHITZ, E. M. 1959 *Fluid Mechanics: Course of Theoretical Physics, vol. 6.* Pergamon.

REICHARDT, H. 1941 Gesetmäßigkeiten der freien Turbulenz. *Z. Angew. Math. Mech.* **21**, 257.

SCHLICHTING, H. 1979 *Boundary-Layer Theory* (7th edn; transl. J. Kestin). McGraw-Hill.

TOLLMIEN, W. 1926 Berechnung turbulenter Ausbreitungsvorgänge. *Z. Angew. Math. Mech.* **6**, 468.

TOWNSEND, A. A. 1976 *The Structure of Turbulent Shear Flow* (2nd edn). Cambridge University Press.

WYGNANSKI, I. & FIEDLER, H. 1969 Some measurements in the self-preserving jet. *J. Fluid Mech.* **38**, 577 (referred to herein as W–F).